expected to remain for at least another 243 days of operation following 5 August 1979. An extended mission has been approved and planning is proceeding to optimize the anticipated scientific bonus.

Multiprobe. Table 1 contains semifinal data on the impact locations of all multiprobe spacecraft (5). These locations are extremely close to the targeting points that were planned before release of the probes from the bus in November 1978.

LAWRENCE COLIN
*Ames Research Center,
Moffett field, California 94035*

References and Notes

1. *Science* **203** (1979), pp. 743–808.
2. L. Colin, *ibid*., p. 743. Since Earth revolves in counterclockwise fashion about the sun in 365.26 days, the synodic period of Venus is 583.92 days, which is thus the time between conjunctions of the Earth-Venus system. Because of the retrograde 243-day rotation period, a Venusian solar day is 116.75 Earth days long, which is almost precisely a factor of 5 less than the synodic period. Thus the same face of Venus is presented to Earth at each interior conjunction.
4. Occultation and eclipse periods are based on tangents at radii of 6139.5 and 6130 km, respectively.
5. These data were obtained as follows. All probes turned on automatically about 22 minutes prior to entry at 200-km altitude and were tracked by the Deep Space Network stations. Trajectory computations were performed at Jet Propulsion Laboratory to provide entry boundary conditions at that altitude. Further computations were performed along a *vacuum* trajectory to 65 km; that is, no atmospheric drag was assumed. The listed impact locations in Table 1 are in fact these 65-km-altitude locations. Future plans call for (i) refining the 200-km-altitude boundary conditions and (ii) providing trajectory computations through a *model* static atmosphere all the way to the surface. Eventually, results of the wind dynamics experiments (differential long-baseline interferometry and the large- and small-probe atmospheric structure experiments) will permit determinations of descent variations from the locations given by the static model.
6. I would like to thank C. F. Hall, J. W. Dyer, and J. R. Cowley, Jr., of the Pioneer Project Office for their review of this report and for obtaining and providing most of the data herein. I would also like to sincerely acknowledge R. W. Jackson, R. O. Fimmel, and J. A. Ferandin for their exceptional efforts at orbiter operation and data processing.

15 May 1979

Thermal Contrast in the Atmosphere of Venus: Initial Appraisal from Pioneer Venus Probe Data

Abstract. *The altitude profiles of temperature and pressure measured during the descent of the four Pioneer Venus probes show small contrast below the clouds but significant differences within the clouds at altitudes from 45 to 61 kilometers. At 60 kilometers, the probe which entered at 59.3° north latitude sensed temperatures 25 K below those of the lower latitude probes, and a sizable difference persisted down to and slightly below the cloud base. It also sensed pressure below those of the other probes by as much as 49 millibars at a mean pressure of 200 millibars. The measured pressure differences are consistent with cyclostrophic balance of zonal winds ranging from 130 ± 20 meters per second at 60 kilometers to 60 ± 17 meters per second at 40 kilometers, with evidence in addition of a nonaxisymmetric component of the winds. The clouds were found to be 10 to 20 K warmer than the extended profiles of the lower atmosphere, and the middle cloud is convectively unstable. Both phenomena are attributed to the absorption of thermal radiation from below. Above the clouds, in the lower stratosphere, the lapse rate decreases abruptly to 3.5 K per kilometer, and a superimposed wave is evident. At 100 kilometers, the temperature is minimum, with a mean value of about 170 K.*

Since our initial report on the atmosphere structure data from the four Pioneer Venus probes (*1*) we have worked toward more precise analysis of the data, filled data gaps, received and interpreted data for an extended altitude range, worked on joining the entry and descent mode data, and attempted initial interpretations of the dynamical significance of the measured contrasts among the probes. The process is still far from complete.

We present here the results for the troposphere in altitude plots to show measured contrasts, discuss the stability of the atmosphere and factors which appear to be affecting it, present improved profiles of the lower stratosphere and compare them with those derived from orbiter remote-sensing (orbiter infrared radiometer experiment). We also discuss some indications of wind oscillations in the upper troposphere. Finally, we make some observations concerning possible dynamical significance of the structure measurements.

The current state of the temperature (T) data is shown in Fig. 1. The descent data from all four probes are shown to a maximum altitude (z) of 66.3 km. Although the first-order result remains that the thermal contrast is small, significant temperature differences are present above 45 km, within the clouds. At the north probe site, the atmosphere is cooler than at the day probe site, by 25 K at 60 km and by 18 K at 50 km. The order of the probes in the upper level temperatures corresponds reasonably to the order of the simultaneously observed infrared radiance at the sites (*2*). Below the clouds, the four curves coalesce to a band with a maximum width of 7 K at 20 km.

All the probes exhibit a temperature offset in the clouds, as compared to the profile below the clouds. This offset is as great as 20 K, defined relative to an extension of the temperature slopes below 40 km. The warming in the clouds is attributed to the absorption of thermal radiation from below as well as to solar absorption, since it occurs on the night probe but to a lesser degree than on the two dayside probes. It is interesting, but probably a result of opposing influences, that the night probe profile tracks the sounder profile very closely at the higher altitudes. The north probe profile, unlike the other three, is warmer than the extended lower atmosphere profile for only a limited altitude range from 40 to 53 km and then cools and drops below it. This may be a consequence of the entry of the north probe into the circumpolar cloud (*3*). Although it is not easy to see in Fig. 1 because of size reduction, there is also a sharp slope change in $T(z)$ at the 270 K levels of all four probes (this slope change is especially noticeable on the sounder profile). It could indicate a phase change in the cloud material, perhaps ice formation, or a change in species beginning at this level (56 to 59 km), which corresponds to the bottom of the upper cloud. [It is noteworthy that 80 percent H_2SO_4 solution freezes at 270 K (*4*).]

The day-night temperature contrast at 30° south latitude is less than 1K at altitudes between 18 and 48 km, that is, below the clouds. A single curve is drawn (Fig. 1) to represent the day and night probes in this range. Below 18 km, the atmosphere at the night probe site is shown to be about 2 K warmer than it is at the day probe site, a somewhat puzzling finding which may be due to inaccuracy. There is work yet to be done in refining these data.

Temperature data in the stratosphere, extending to 110 km, are also shown for the north and day probes in Fig. 1. These were obtained from deceleration measurements during high-speed entry (*1*) and have now been better joined to the descent data. To a first approximation, altitude and velocity are matched at the intersection of entry with descent measurements. The wave structure suggested in (*1*) is still present, with an amplitude of about ±20 K. The waves at the two entry sites are out of phase at an altitude of 97 km. The temperature minimum, including the wave minimum, is 160 K, whereas the minimum in the mean profile might be ~170 K. The atmospheric densities determined from entry mode data in the altitude range from 60 to 64 km (north probe) and 65 to 69 km (day probe) are affected by the presence of winds. Entry mode temperatures at these altitudes are still uncertain and are omitted.

Comparison is shown in Fig. 1 of these profiles with the remote infrared soundings from Pioneer orbiter, indicated by the two dashed curves, each defined by four data points taken at appropriate latitudes from figure 2 of (*3*). The restriction to four points requires a smooth fairing, but the infrared data may give a fundamentally smoother approximation as a result of averaging over finite altitude spans. The infrared temperatures are perhaps 10° higher than a mean curve through our data between 75 and 95 km. The atmospheric density is 10^{-5} kg/m³ at 106 km, increasing to ~ 0.4 kg/m³ at 60 km, in slightly wavy profiles. The density ratio of the day probe to the north probe is near unity at 84 and 105 km but increases to 1.5 at 95 km.

The atmospheric pressure (p) data taken by the four probes during descent are plotted in Fig. 2 against derived altitudes. The temperature differences result in measurable pressure differences above 34 km, which become very large at the higher levels. At 60 km, for example, the difference between the north probe and the day probe is 49 mbar at a mean pressure of 200 mbar. Three of the data sets are clustered at cloud levels to within a few percent of pressure. The north probe data set diverges from the other three. The day-night differences are of the order of 4 mbar at 100 mbar, 6 mbar at 200 mbar, 26 mbar at 400 mbar, and 20 mbar at 1000 mbar (comparable to pressure differences on Earth), with the higher pressures at the morning terminator. At the sounder location, upper lever pressures are closely comparable to those at the night location.

Below 40 km the north and night probe data still differ by about 4 percent (0.2 bar at 5 bars), but below 30 km a single curve, drawn through the sounder data, represents all the data, typically within 1 percent. Pressure differences at touchdown were interpreted as elevation differences (*1*), and all altitudes are referenced to the sounder landing site.

We have considered the possible influence of altitude errors on these comparisons. Below 30 km, it appears that the correspondence of the four data sets would be a highly improbable coincidence, and that altitude is determined to better than our estimated accuracy of 1 percent, or 0.3 km at 30 km. This correspondence builds confidence that the differences at the higher levels are real, but the possibility remains that details of the comparisons could be altered by further refinements in the determination of altitude.

The local atmospheric static stability against overturning, calculated from the sounder pressures and temperatures, is plotted in Fig. 3 as a function of pressure. The adiabatic lapse rate (Γ) is for an atmosphere consisting of 96.5 percent CO_2 and 3.5 percent N_2 (*5*, *6*). As we reported earlier (*1*), much of the atmosphere is statically stable, except for an unstable layer in the middle cloud (*7*, *8*) at 50 to 55 km. There appears to be another local region of instability at 20 to 28 km. (A more recent evaluation shows that this latter layer may be close to neutrally stable.) The destabilizing trend which results in instability in the clouds begins just below the lower cloud, possibly a result of precloud layers or increased water vapor (*5*). The relatively high stability at 49 km corresponds almost exactly with the gap between the lower cloud and the middle cloud. Thus, the clouds appear to be controlling the static instability at the upper levels. The uppermost cloud (above 56 km) does not

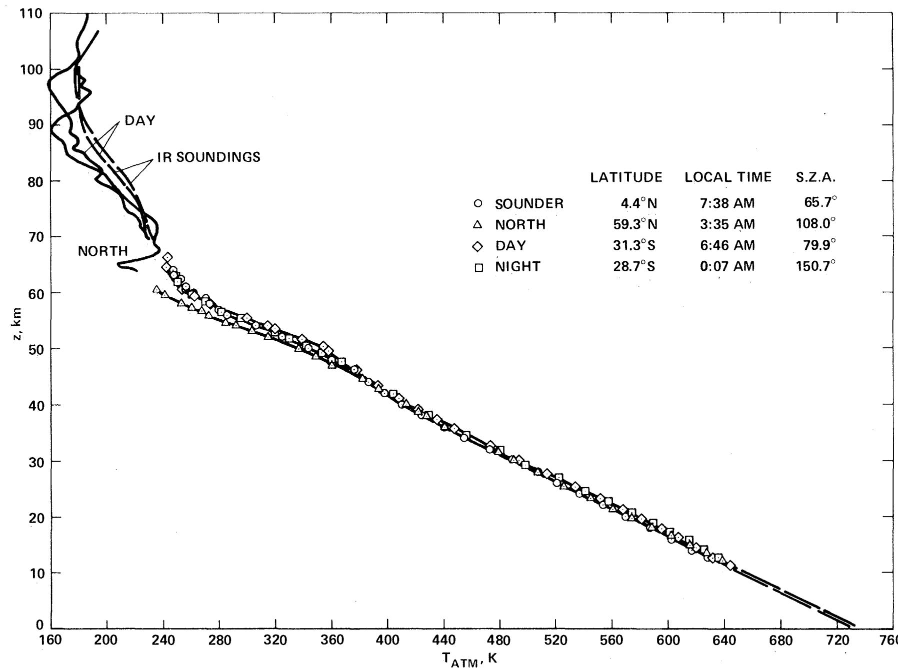

Fig. 1. Temperature profiles in the atmosphere of Venus from four Pioneer Venus probes. Abbreviations: *IR*, infrared; *S.Z.A.*, solar zenith angle. Data below 65 km are from direct sensing; data above 65 km are from measurements of probe deceleration. Altitudes were reconstructed for each probe from the equation of hydrostatic equilibrium (*1*).

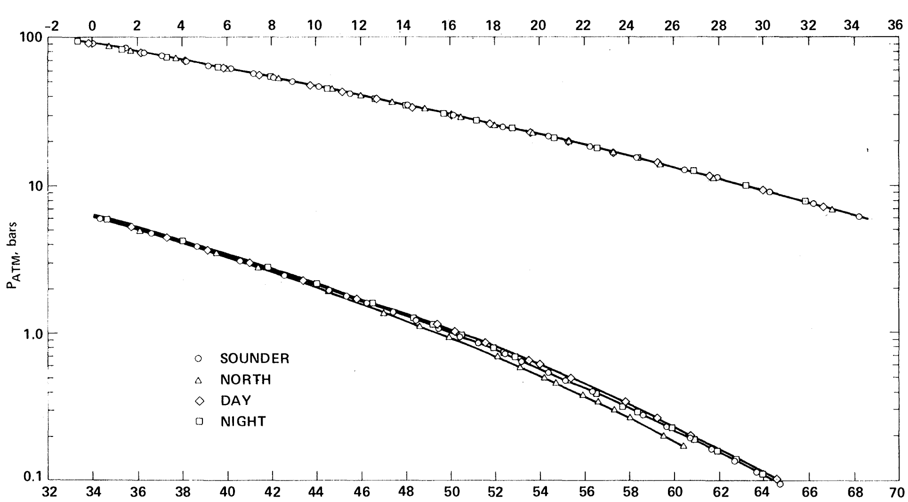

Fig. 2. Pressure profiles. Below 30 km, the four probes define a single variation; at higher altitudes, sizable differences develop. Altitudes are referred to the sounder landing elevation.

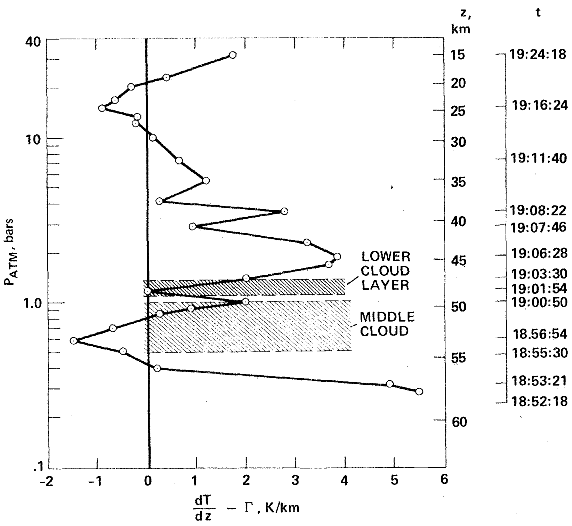

Fig. 3. Static stability of the atmosphere against overturning. Negative values indicate instability. The atmosphere is stably stratified except for limited regions, one of which is in the dense cloud. Digital resolution uncertainty (~1 K/km) could affect the magnitude of instability, but not the general character of the variation.

produce instability, however, probably because it is too tenuous. The instability in the middle cloud is probably one source of the turbulence measured by Mariners 5 and 10 (*9*) and could be related to convection cells seen in the clouds in the ultraviolet photographs (*10*). The convection cells in the photographs are, however, of very large scale compared to the depth of the unstable layer in the clouds.

The stability diagram for the small probes was the same qualitatively and about the same quantitatively as that plotted in Fig. 3, including both probes entering on the nightside of the planet. Thus, solar energy deposition cannot be the mechanism leading to instability in the clouds. The most likely mechanism is absorption by the clouds of thermal radiation from below (*11*).

The unstable region around 15 bars also appears on the small probes, although the details differ somewhat from probe to probe. At pressures exceeding 40 bars we did not compute the stability since the temperature measurements were lost in this region (*1*).

The pressure differences in Fig. 2 are primarily but not entirely meridional. We have interpreted these differences to define zonal flow velocities as a function of altitude, based on the assumption of cyclostrophic balance, in which the pressure difference balances the meridional component of the centrifugal acceleration due to the zonal wind, U_w (*12*). Then, under the assumption of constant zonal flow velocity (*13*) at a given altitude (over the colatitude interval θ_1 to θ_2), the equation

$$U_w^2 = (\Delta p/\bar{p})R\bar{T}/(\ln \sin \theta)_{\theta_1}^{\theta_2} \quad (1)$$

relates the observed meridional pressure difference Δp to the velocity (*14*). Here, $\bar{p}$ and $\bar{T}$ are, respectively, the mean pressure and the mean temperature across the interval at this altitude, and R is the gas constant, 190.3 J kg^{-1} K^{-1}. Pressures at north and south latitudes are for this purpose assumed to be symmetrical about the equator.

Equation 1 is applied to pressure differences between two probes, one of which is always the north probe, to obtain the wind velocities in Fig. 4. The three profiles obtained agree to within about ± 20 m/sec, which is a measure of neglected contributions of other terms in the complete equation of motion, variability of winds over the planet, and errors in the data. The profiles may be compared with the initial wind measurements of the Pioneer Venus differential long-baseline interferometer (DLBI) experiment (*15*) and with the Venera 8 data (*16*). The indication is that cyclostrophic balance is approximately satisfied and is the major source of meridional pressure difference between 40 and 65 km.

That the other advective terms in the meridional momentum equation are not negligible, however, is indicated by the

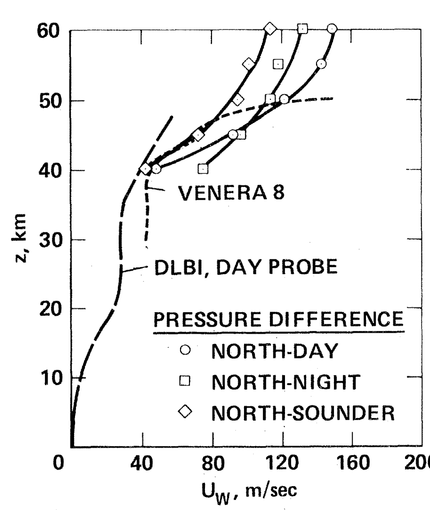

Fig. 4. Zonal winds deduced from the measured pressure differences, under the assumption of cyclostrophic equilibrium.

pressure difference between +4° and −30° latitude (the sounder and day probes), which is opposite in sense to that required for cyclostrophic balance and implies flow toward the equator at 40 to 65 km in the southern hemisphere (*17*), and by the day-night pressure difference at almost the same latitude measured by the day and night probes. Since the mean meridional wind velocities are indicated to be small compared to the mean zonal wind (*13*), one is led to the conclusion that significant planetary scale nonaxisymmetric motions are present at latitudes below about 30°. Such a conclusion is consistent with the day-night pressure difference. On the basis of the curves in Fig. 1, this eddy activity may extend into the lower atmosphere.

A further interesting feature of Fig. 2 is that the day probe exhibits an inflection in $p(z)$ between 1.7 and 1.9 bars, such that the day-night probe pressure difference changes phase. Such a crossover implies either a height-dependent phase or perhaps places where there are nodes in the amplitudes of the waves or eddies.

There have been several other indications of flow oscillations in the lower atmosphere. The mean axial accelerations of all four probes show small-amplitude, long-period oscillations that may indicate vertical or horizontal flow oscillations. On the sounder, the deepest of these occurs at an altitude of 9.5 km, with another at about 21 km. On the night probe, these are accompanied by quieting of the unsteadiness in the acceleration. On the north probe, the trajectory reconstruction in descent has revealed long-period (3- to 5-minute) oscillations in the Doppler residuals, corresponding in one instance to a vertical wavelength of 5.2 km. These observations support the inference of wave motions in the lower atmosphere.

ALVIN SEIFF, DONN B. KIRK
RICHARD E. YOUNG, SIMON C. SOMMER
NASA Ames Research Center, Moffett Field, California 94035
ROBERT C. BLANCHARD
NASA Langley Research Center, Hampton, Virginia 23665
JOHN T. FINDLAY, G. M. KELLY
Analytical Mechanics Associates, Hampton, Virginia 23666

References and Notes

1. A. Seiff *et al.*, *Science* **203**, 787 (1979).
2. J. Apt and R. Goody, *ibid.*, p. 785.
3. F. W. Taylor *ibid.*, p. 779.
4. W. F. Giauque, E. W. Hornung, J. E. Kunzler, T. R. Rubin, *J. Am. Chem. Soc.* **82**, 62 (1960).
5. V. I. Oyama, G. C. Carle, F. Woeller, J. B. Pollack, *Science* **203**, 802 (1979).
6. A. T. Young has suggested [*Geophys. Res. Lett.* **6** (No. 1), 49 (1979)] that there could be relatively large abundances of polyatomic sulfur molecules in the lower atmosphere, which could

affect this presentation at the lower altitudes.
7. R. G. Knollenberg and D. M. Hunten, *Science* **203**, 792 (1979).
8. B. Ragent and J. Blamont, *ibid.*, p. 790.
9. R. Woo and W. B. Kendall, *J. Atmos. Sci.* **31**, 1698 (1974); R. Woo, *ibid.* **32**, 1084 (1975).
10. L. D. Travis, D. L. Coffeen, J. E. Hansen, K. Kawabata, A. A. Lacis, W. A. Lane, S. S. Limaye, P. H. Stone, *Science* **203**, 781 (1979).
11. Although the release of latent heat could also be important in determining thermal structure (and, therefore, convective instability) within the clouds, we believe thermal radiation from below is the primary mechanism. First, the onset of the warming and in fact almost the entire thermal offset of the clouds, discussed in the text relative to Fig. 1, occurs at 40 to 50 km, that is, below the clouds, where latent heat release cannot be a factor. Furthermore, to duplicate the magnitude of the divergence in the net upward infrared flux [R. W. Boese, J. B. Pollack, P. M. Silvaggio, *Science* **203**, 797 (1979)] by latent heat release within the clouds requires that all of the droplets be transported to lower altitudes for vaporization and regenerated on a time scale of 5000 seconds. This should be accompanied by a growth in total droplet mass per unit volume with height, which is not seen in the data (*7*).
12. C. B. Leovy, *J. Atmos. Sci.* **30**, 1218 (1973).
13. V. E. Suomi, *NASA Spec. Publ. 382* (1974).
14. The magnitude of the derived wind depends on the distribution $U_w\theta$ assumed. Thus, for example, for solid body rotation, equatorial velocities are increased by about 50 percent.
15. C. C. Counselman III, S. A. Gourevitch, R. W. King, G. B. Loriot, *Science* **205**, 85 (1979).
16. M. Ya. Marov *et al.*, *J. Atmos. Sci.* **30**, 1210 (1973).
17. This is consistent with the wind measurement at the day probe site (*15*). Furthermore, this pressure difference becomes small at the altitude (~40 km) where the measured wind velocities become small.
18. We thank O. B. Toon for helpful discussions concerning the relative importance of latent heat release and infrared radiation in the maintenance of the thermal structure in the clouds. We thank L. Pfister for many helpful discussions concerning the dynamical implications of the data.

15 May 1979

Composition and Structure of the Venus Atmosphere: Results from Pioneer Venus

Abstract. *Results from the Pioneer Venus sounder probe neutral mass spectrometer indicate that there is no difference in the isotopic ratios of carbon and oxygen between Venus and Earth to within ± 5 percent. The mixing ratio of nitrogen is* 3.5^{+3}_{-2} *percent with an isotopic ratio within 20 percent of that of Earth. The ratio of argon-36 to argon-40 is 85 percent, and the ratio of argon-38 to argon-36 is 20 percent. The mixing ratios of argon-36 and argon-40 are approximately 40 and 50 parts per million, respectively, with an error of about a factor of 2 (mainly toward a lesser amount) resulting from uncertainty in the response of the ion pump to rare gases. Hydrogen chloride cannot account for more than a few percent of the 36 mass peak, and therefore the large excess of primordial argon is a reasonable conclusion. The ratio of neon-20 to argon-36 of 0.5 ± 0.3 is definitely terrestrial in character rather than solar. These results indicate that there is a large excess of all primordial noble gases on Venus relative to Earth. There appears to be a considerably higher abundance of sulfur compounds below 20 kilometers than in or above the main cloud layer. The 32 and 60 mass peaks show a sharp increase below 22 kilometers, indicating the possible production of sulfur and carbon oxysulfide (COS) at the expense of sulfur dioxide.*

The mass spectrometer on the Pioneer Venus sounder probe, which entered the Venus atmosphere on 9 December 1978 (*1*), measured the atmospheric composition relative to CO_2, the dominant constituent, from an altitude of 61 km to the surface. The instrument, a single-focusing, magnetic-sector spectrometer (*2*), scanned the mass range from hydrogen through mercury with a dynamic range of six decades. Because the instrument was designed to measure atmospheric composition rather than density, a gate valve (*3*), operated by the increasing atmospheric pressure encountered during descent, was installed to control the ion source pressure to a relatively constant value as the inlet leak throughput continually increased. The result was as follows: (i) a sensitivity of 1 part per million (ppm) was attained throughout most of the descent while the atmospheric pressure changed by four orders of magnitude and (ii) the instrument output signals are not related directly to atmospheric density but are relative to CO_2. Figure 1 is the altitude profile of CO_2 in terms of instrument output signal (related to counting rate). Since this is not a density profile but a measure of the partial pressure of CO_2 in the ion source, all other data will be presented as mixing ratios relative to this CO_2 profile.

The decrease in signal starting at 51 km is caused by a blockage of the inlet leak, which occurred after the probe passed through most of the cloud layer designated region C of the nephelometer data (*4*). This blockage occurred presumably as a result of an overcoating of cloud materials (hydrated H_2SO_4 droplets) which lasted until the probe emerged from the lower haze layer at 31 km (*5*), at which time the flow of atmospheric gases resumed.

The isotopic ratios of C and O, ^{13}C to ^{12}C, and ^{18}O to ^{16}O have been found to be close to Earth values. The C ratio from the CO_2^{2+} peaks at mass 22 and 22.5 is about 0.012, approximately 5 percent higher on Venus than on Earth, with a standard deviation of ± 5 percent. The 45/44 mass peak ratio (CO_2^+) yields, on the average, a similar number. The $^{18}O/^{16}O$ ratio was within 1 percent of the Earth value (0.00204), also with a standard deviation of ± 5 percent.

In order to determine the N_2 abundance on Venus from the mass spectrometer data, several methods were used. Because of the rather large production of CO from CO_2 in the ion source, the 28 mass peak is comprised of both CO^+ and N_2^+ (the majority being CO^+). The CO^+ peak amplitude is a function of the degree to which the gate valve to the ion source pump (a chemical getter pump) was open, and its ratio to CO_2^+ varied from 0.4 when the valve was closed to 0.12 when the valve was wide open. On the basis of data from the lowest part of the descent profile and corrections for the CO contribution, the N_2 mixing ratio was found to be approximately 2.5 percent. However, the uncertainty in the result is fairly large, at least 50 percent.

A second method is to derive the N_2 content from the 29/28 mass peak ratio. If the nitrogen isotopic ratio is equivalent to that in Earth's atmosphere and if the 29 mass peak consists entirely of the ^{13}C and ^{15}N isotopic peaks (which does not appear to be true between 20 and 5 km), the N_2 mixing ratio was found to be 3 percent below 5 km and approximately 4 percent above the dense cloud layer. The uncertainty is of the order of 50 percent. Because of the magnitude of the uncertainties, there is no implication in these numbers that the atmosphere is anything but well mixed. If the nitrogen isotopic ratio were increased by 20 percent, the N_2 mixing ratio would increase by 1.5 percent. For a 70 percent increase in the $^{15}N/^{14}N$ ratio, as was found on Mars (*6*), the 29/28 mass ratios for both C and N would become equal and it would be impossible to determine the N_2 abundance by this method. However, since the 29/28 mass peak ratio is 0.103, the maximum allowed enhancement in the $^{15}N/^{14}N$ ratio would be 35 percent. This value would require the entire 28 mass peak to be N_2, which it clearly cannot be. It therefore appears that the most probable value of the nitrogen isotopic ratio is close to that on Earth.

The third method for determining the N_2 abundance is based on the peak at 14 atomic mass units (amu), which consists of a mixture of ^{14}N, CH_2 from methane, and CO^{2+} and N_2^{2+}. If corrections are made for methane and doubly charged

0036-8075/79/0706-0049$00.75/0